



# Growing up gator: a proteomic perspective on cardiac maturation in an oviparous reptile, the American alligator (*Alligator mississippiensis*)

Sarah L. Alderman<sup>1</sup> · Dane A. Crossley II<sup>2</sup> · Ruth M. Elsey<sup>3</sup> · Todd E. Gillis<sup>1</sup>

Received: 29 October 2019 / Revised: 22 December 2019 / Accepted: 9 January 2020  
© Springer-Verlag GmbH Germany, part of Springer Nature 2020

## Abstract

We recently described lasting changes in the cardiac proteome of American alligators (*Alligator mississippiensis*) reared under hypoxic conditions, that resemble what embryos encounter in natural nests. While these changes were consistent with functional differences in cardiac performance induced by developmental hypoxia, the magnitude of this response was dwarfed by a much greater effect of development alone (76% of the total differentially abundant proteins). This means that substantial differences in relative steady-state protein expression occur in the hearts of alligators as they mature from egg-bound embryos to 2-year-old juveniles, and this developmental program is largely resistant to variation in nest conditions. We therefore performed functional enrichment analysis of the 412 DA proteins that were altered by development but not hypoxia, to gain insight into the mechanisms of cardiac maturation in this ectotherm. We found that the cardiac proteome of alligators at 90% of embryonic development retained a considerable capacity for transcription and translation, suggesting the heart was still primarily invested in growth even as the animal approached hatching. By contrast, the cardiac proteome of 2-year-old juveniles was weighted towards structural and energetic processes typical of a working heart. We discuss our results in the context of differences in cardiac development between ectothermic and endothermic oviparous vertebrates, and argue that the robust developmental program of the alligator heart reflects a slow-paced ontogeny, unburdened by the requirement to support the elevated peripheral oxygen demand typical of endothermic animals from a young age.

**Keywords** Heart · Reptile · Oxygen · iTRAQ · Developmental programming · Phenotypic plasticity

## Introduction

The heart is among the first organs to become functional in developing vertebrates, reflecting its pivotal role in circulating oxygen, nutrients, and metabolic wastes among developing tissues. Yet, while the heart functions as a pump in early development, the structure of myocytes and the whole heart

undergo considerable morphological changes during maturation, and the mature cardiac phenotype is not achieved until well into postnatal life. This means that while the embryonic heart serves as a convective pump, it is simultaneously laying the scaffold for, and supporting, its own maturation. This maturation has been well studied in mammals and includes: molecular modifications to the complement of protein isoforms expressed, including components of the troponin complex (Posterino et al. 2011; Racca et al. 2016; Dykes et al. 2018), morphological changes to cardiomyocytes including the appearance of T-tubules (Hoerter et al. 1981; Nakanishi and Jarmakani 1984), and improved metabolic efficiency including increased capacity for oxidative phosphorylation as well as a switch in fuel preference from carbohydrates to fatty acids (Lopaschuk and Jaswal 2010). The result is a functional shift towards improved contractile capacity of the myocytes (Fabiato and Fabiato 1978; Anderson et al. 1984; Tibbits et al. 2002; Posterino et al. 2011). For example, heart mass, cardiac mitochondrial volume, and cardiomyocyte

Communicated by H. V. Carey.

✉ Sarah L. Alderman  
alderman@uoguelph.ca

<sup>1</sup> Department of Integrative Biology, University of Guelph, 50 Stone Road E, Guelph, ON N1G 2W1, Canada

<sup>2</sup> Developmental Integrative Biology Research Group, Department of Biological Sciences, University of North Texas, Denton, TX 76203-5017, USA

<sup>3</sup> Louisiana Department of Wildlife and Fisheries, Rockefeller Wildlife Refuge, Grand Chenier, LA 70643, USA

contractile machinery increase substantially as marsupial neonates become endothermic in preparation for leaving the maternal pouch (Snelling et al. 2015a, b).

In eutherian mammals, parturition is a major stimulus to switch from the fetal to adult cardiac phenotype. At birth, blood pressure and oxygen partial pressure ( $PO_2$ ) of arterial blood rapidly increase as gas exchange is diverted from placental circulation to the lungs (Berger et al. 1990). This supports the increased metabolic demands of heat-generating organs (e.g., skeletal muscle) as the animal becomes endothermic (McManus 1971; Goldspink and Ward 1979; Hulbert 1988; Agbulut et al. 2003; Gokhin et al. 2008; Robertson et al. 2019). The heart is central to these physiological changes as it drives the convection of oxygen and metabolic fuels that enable enhanced aerobic capacity. In air-breathing oviparous vertebrates, such as birds and reptiles, hatching also causes an increase in blood  $PO_2$  as gas exchange transitions from the chorioallantoic membrane to the lungs (Thompson 2007). As in mammals, the hearts of reptiles and birds mature after hatch into the adult phenotype. However, when comparing the maturation of reptile and bird hearts, one needs to consider the differences in the functional requirements of the adult cardiovascular systems. One obvious difference is that as endotherms, birds have a higher resting metabolic rate ( $MO_2$ ) that requires a greater capacity for oxygen delivery to the tissues. At the level of the heart, this translates into greater cardiac output and pressure, as well as a higher metabolic capacity (Mortola and Labbè 2005; Sirsat et al. 2016a, b). Soon after birds hatch, and coincident with the onset of endothermy, there is a rapid increase in relative heart mass coupled with mitochondrial biogenesis and a switch from carbohydrates to fatty acids as a metabolic fuel (Walter and Seebacher 2009; Sirsat et al. 2016a). Free of such metabolic demand, the heart of ectotherms likely undergoes a more subtle maturation. Indeed, relative heart mass and cardiomyocyte oxidative phosphorylation capacity are stable for at least 1 month post-hatch in alligators and common snapping turtles (*Chelydra serpentina*) (Sirsat et al. 2016b).

The purpose of this study was to examine maturation of the reptile heart by characterizing the differences in the cardiac proteome between embryonic and 2-year-old American alligators (*Alligator mississippiensis*). It was predicted that the cardiac proteome of the juvenile alligators would reflect an increase in aerobic capacity and relative contractile function, compared to that of embryonic alligators. We recently demonstrated that alligators exposed to low levels of oxygen during embryogenesis experience a considerable shift in the cardiac proteome, and that these changes in relative steady-state protein expression are carried forward into later life stages (Alderman et al. 2019). Remarkably, the effects of developmental hypoxia on the cardiac proteome existed against a backdrop of a substantially greater ontogenic shift

in steady-state protein expression. This suggests a robust developmental program that is highly resistant against environmental perturbations, and therefore likely to be critical for normal cardiac development. Here, we detail how steady-state protein expression changes in the heart of American alligators as they transition from egg-bound embryos to free-living juveniles, and consider these changes under the themes of alligator life history as well as the evolution of endothermy.

## Methods

### Animals

Full experimental details are available in (Alderman et al. 2019). Briefly, American alligator (*Alligator mississippiensis*) eggs were collected from a total of eight nests at the Rockefeller Wildlife Refuge (Grand Chenier, LA) and transported to the University of North Texas (Denton, TX) for initial staging and experimentation. Eggs were randomly placed in plastic containers containing a 1:1 vermiculite:water mixture, and incubated at 30 °C to ensure that all embryos developed as females. At approximately 20% of incubation (total incubation time is 72 days at 30 °C), eggs were incubated at either 21% oxygen (normoxia) or 10% oxygen (hypoxia) in keeping with natural conditions in crocodilian nests (Lutz and Dunbar-Cooper 1984). At 90% of incubation, four clutch-matched eggs from each condition were removed from incubation, euthanized using isoflurane, and the heart ventricle was excised and flash-frozen. The remaining eggs were allowed to hatch, at which point the hatchling alligators were marked by tail scute clipping and photographed to identify the incubation condition and clutch of origin. All animals were maintained under identical conditions for 2 years, at which time they were euthanized via isoflurane and heart ventricles were excised and flash-frozen. All samples were stored at − 80 °C until processing. The experiments were approved by the University of North Texas animal ethics committee IACUC (#17-001) in accordance with AWA regulations.

### Proteome quantitation

The heart ventricles from 15 alligators ( $n=4$  each for embryos in normoxia and hypoxia;  $n=4$  juvenile normoxia;  $n=3$  juvenile hypoxia) were processed for proteome quantitation and characterization using isobaric tags for relative and absolute quantitation (iTRAQ), as described in (Alderman et al. 2019). Briefly, 200 µg of extracted proteins from each tissue sample were denatured and reduced, then cysteine residues were blocked prior to overnight digestion by trypsin (Promega Corporation, Madison, WI). Digested

peptides were labeled using two 8-plex iTRAQ kits (SCIEX, Framingham, MA) according to manufacturer's instructions, with one sample (embryo, normoxia) labeled in replicate reactions to serve as an internal control on the two plexes. Labeled peptides were pooled into their respective 8-plexes and analyzed by mass spectrometry at SickKids Proteomics Analysis Robotics & Chemical Biology Centre (Toronto, ON) as previously described (Alderman et al. 2017). Identification and quantification of cardiac proteins were performed using Proteome Discoverer v2.2.0.388 (ThermoFisher, Waltham, MA), and mass spectra were searched against the NCBI non-redundant protein database (March 8, 2018) using the following spectrum file search settings: 20 ppm precursor mass tolerance, 0.5 Da fragment mass tolerance, carbamidomethylation and iTRAQ static modifications, at least two unique identifying peptides, and target false discovery rate (FDR) 5%. Protein abundances were normalized to total protein in each run and missing values imputed by low abundance re-sampling. Data were scaled to the internal control sample to allow direct comparison between the two plexes. Only proteins that were identified on both plexes were considered for bioinformatics analysis.

## Bioinformatics analyses

The software platform Perseus (Tyanova et al. 2016) was used to determine differentially abundant proteins using two-way ANOVA (FDR = 5%) and Benjamini–Hochberg correction for multiple hypothesis testing, with *age* (embryo, juvenile) and *oxygen* (normoxia, hypoxia) as main factors and allowing for their interaction (*age* × *oxygen*). Pairwise group comparisons were made using Tukey's honestly significant difference post hoc test on significant ANOVA hits ( $q < 0.05$ ). To understand the effect of development on the cardiac proteome, functional enrichment analysis was carried out on the subset of differentially abundant proteins that was uniquely altered by the main effect of age, in STRING (<https://string-db.org>; May 27, 2019) using the human orthologues of gene names and setting the identifying organisms to *Homo sapiens*. Visualizations of enriched pathways were achieved using ReviGO (<https://revigo.irb.hr>) and Cytoscape (<https://cytoscape.org/>) to reduce redundancy and bias from data interpretation.

## Results

### Proteome characterization and differential expression analysis

The spectral reads from the two 8-plex iTRAQ experiments were assigned to 2405 protein identifications, of which 99 were removed as common or blood contaminant proteins

(ex. keratin, albumin), 1084 were only represented on one of the two 8-plex experiments, and 318 were identified by only 1 unique peptide. The spectral reads for the remaining 904 high-confidence protein identifications had, on average, 24% sequence coverage and 7.5 unique peptide identifications. The full dataset is freely available using the identifier PXD013974 on ProteomeXchange (<https://www.proteomexchange.org/>).

The relative abundances of 557 proteins were altered by the experimental conditions, of which 521 were significantly altered by *age*, representing 58% of the quantified proteome. The subset of differentially abundant (DA) proteins that was unique to *age* and independent of any effect of *oxygen* was defined by 412 proteins (Fig. 1a), with 31 proteins having an absolute fold change (FC) greater than 1.5 (Fig. 1b, c). The top four up- and down-regulated proteins ranged 1.7–2.1 absolute FC (Fig. 1d). To maximize input for functional enrichment analyses, those proteins with  $q < 0.05$  and absolute  $FC_{\text{juvenile:embryo}} > 1.2$  (Fig. 2a) were considered in functional enrichment analyses. The DA proteins that fit the above criteria included 78 up-regulated and 97 down-regulated proteins, for a total of 175. Human orthologues for 75 of 78 up-regulated proteins, and for 95 of 97 down-regulated proteins were recognized by STRING and used to inform network and functional analyses. Known interactions among the up- and down-regulated proteins were visualized as protein–protein interaction (PPI) networks, with interaction score set to high confidence (0.700), unconnected nodes hidden from view, and network clustering using the MCL algorithm. Both sets of DA proteins yielded significantly more interactions than would be expected from a random set of proteins of similar size (PPI enrichment  $p$  values were  $2.44 \times 10^{-10}$  and  $< 1.0 \times 10^{-16}$  for up- and down-regulated protein sets, respectively); however, there were substantial differences in the number of nodes present in each network. While 27 nodes (or 36% of inputted proteins) defined the PPI network for the up-regulated DA proteins (Fig. 2b), the number of nodes more than doubled to 63 (or 66% of inputted proteins) for down-regulated DA proteins (Fig. 2c).

### Gene ontology (GO) analysis

In general, enrichment of GO terms was greater for down-regulated than for up-regulated proteins, both in terms of the number of significantly enriched terms and in their functional relatedness (Supplemental Data File S1). For biological processes, a total of 136 GO terms were enriched, with 34 and 108 for each of up- and down-regulated proteins, respectively. The six shared terms between the two sets of DA proteins included organonitrogen compound metabolic process, organelle organization, cellular component organization, cellular component organization or biogenesis, intracellular transport, and fatty acid

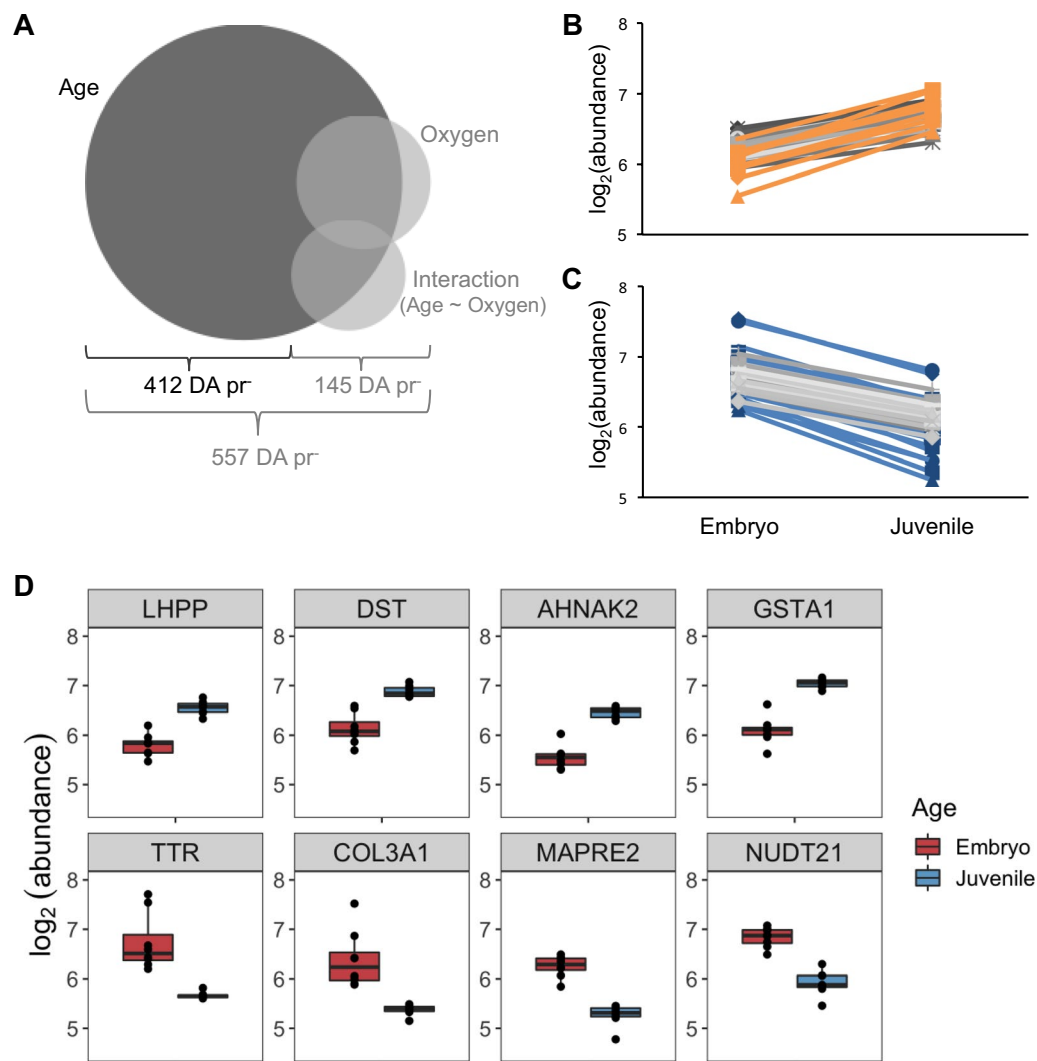


**Fig. 1** Summary of differentially abundant proteins. **a** Venn diagram showing the relative proportions of the differentially abundant proteins (DA pr<sup>-</sup>) among the experimental treatments. The 412 DA pr<sup>-</sup> unique to the main effect of developmental age (dark grey) were pared to include only those with an absolute fold change greater than 1.2. There were 78 up-regulated (**b**) and 97 down-regulated (**c**) proteins in total, with 9 (yellow) and 22 (blue) having an absolute fold change greater than 1.5. **d** Boxplots of the top four up- and down-regulated

proteins in embryo (red;  $n=8$ ) and juvenile (blue;  $n=7$ ) heart ventricles. *LHPP* phospholysine phosphohistidine inorganic pyrophosphate phosphatase, *DST* dystonin, *AHNAK2* protein AHNAK2, *GSTA1* glutathione S-transferase A1, *TTR* transthyretin, *COL3A1* collagen type III alpha 1, *MAPRE2* microtubule-associated protein RP/EB 2, *NUDT21* cleavage and polyadenylation specificity factor subunit 5 (color figure online)

beta-oxidation. Functional networks generated from these enriched GO terms were generally sparse for up-regulated proteins, but grouped into two themes: organization and metabolism (Fig. 3a). In contrast, one densely populated and two smaller networks were generated from GO terms enriched by down-regulated proteins (Fig. 3b). The largest was a 29-node network containing 238 edges (network density = 29%, determined as the number of actual edges relative to the number of possible edges), with the most influential nodes (highest number of edges) relating to translation and transcription (13–18 edges/node). The two smaller networks related to transport processes (nine

nodes; network density = 100%) and organization (six nodes, network density = 100%).

For Cellular Components, a total of 90 GO terms were enriched, with 40 and 58 terms for each of up- and down-regulated proteins, respectively. Among the 18 GO terms that were shared between the two sets of DA proteins, enrichment typically weighted more heavily towards down-regulated DA proteins compared to up-regulated DA proteins (Fig. 4). Functional networks generated from these enriched GO terms indicate a high level of relatedness. A redundancy-reduced network consisting of 20 nodes and 102 edges (network density = 27%) was generated for

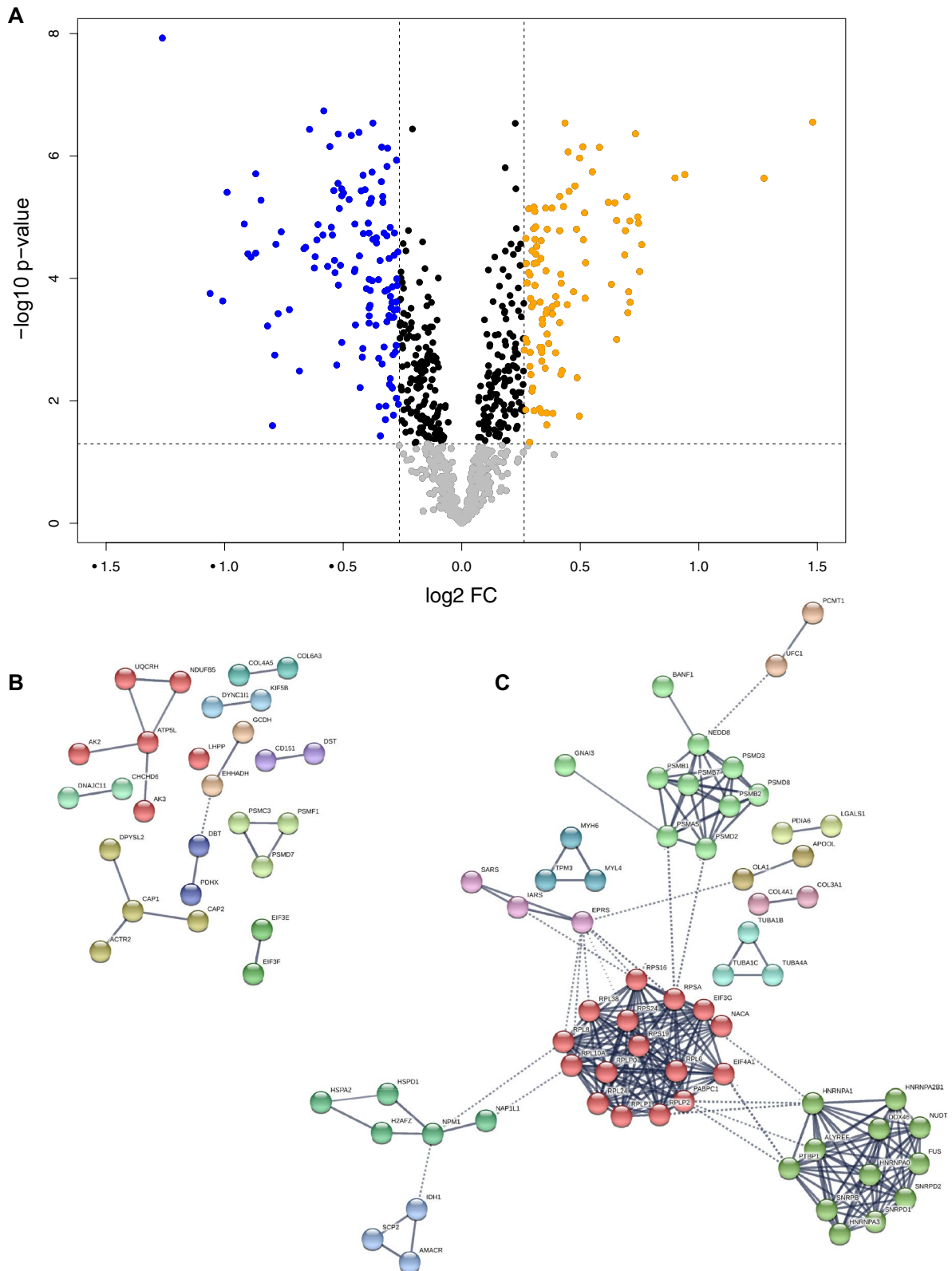


**Fig. 2** **a** Volcano plot of protein abundances, shown as the inverse log of the  $p$  value ( $-\log_{10} p$  value) versus  $\log_2$  fold change (FC). The cutoffs for proteins used in network analyses were 1.2 FC and  $p < 0.05$ , and highlighted separately for up-regulated (yellow) and

down-regulated (blue) proteins. Protein interaction networks were generated separately for up-regulated (**b**) and down-regulated (**c**) proteins, using default parameters in STRING. Colors define related protein clusters (color figure online)



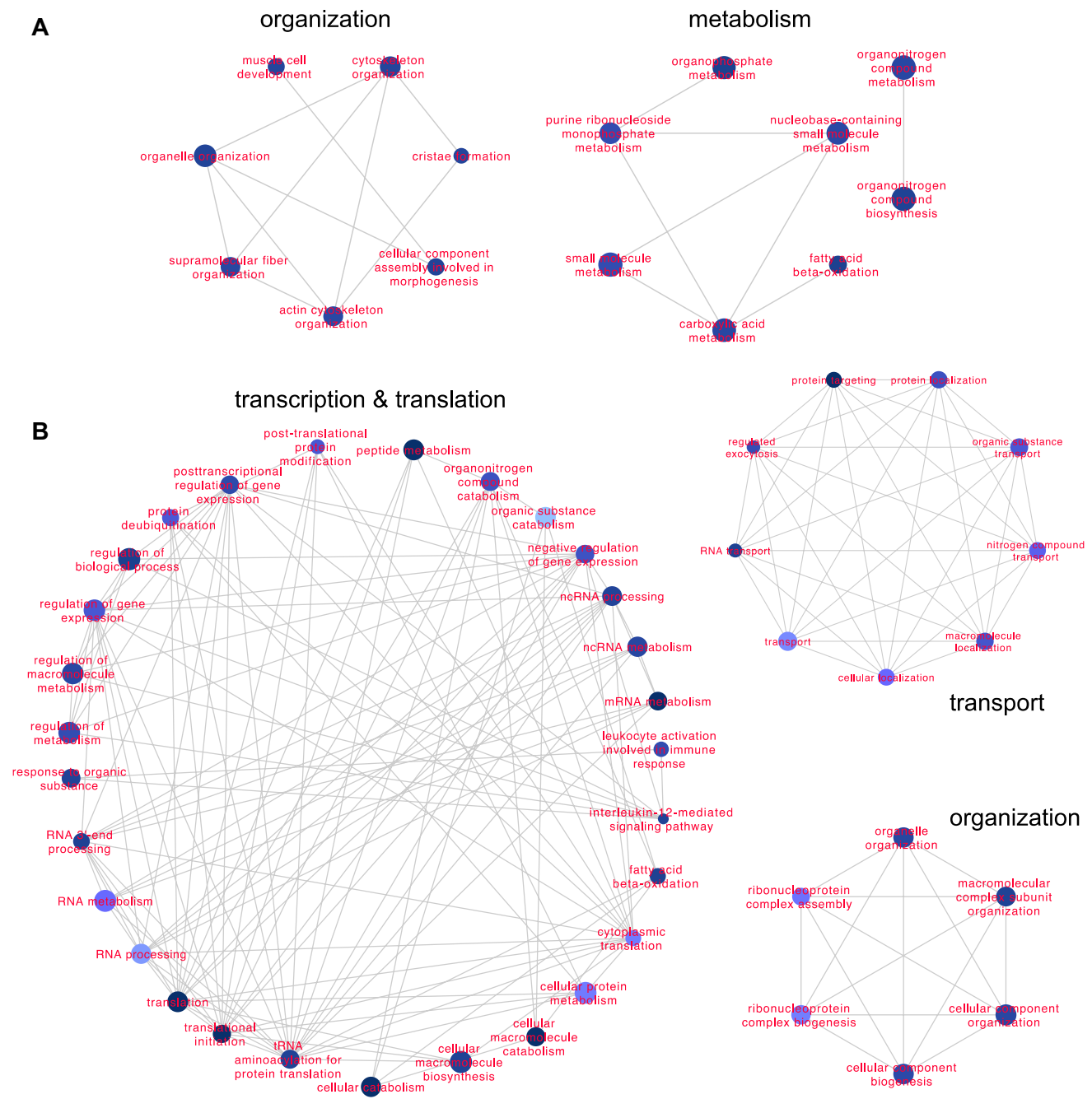


**Fig. 3** Functional networks of enriched GO terms within Biological Processes for proteins that were (a) up-regulated and (b) down-regulated in juvenile relative to embryonic hearts

down-regulated DA proteins, and revealed the most influential nodes as catalytic step 2 spliceosome, cytosolic ribosome, polysomal ribosome, and ribosomal subunit (Fig. 4). In fact, the dominant theme amongst nodes in this network was effectors of RNA processing. For up-regulated DA proteins, the same visualization approach generated a network of 17 nodes connected by 96 edges (network density = 35%), where top influential nodes included podosome and mitochondrial protein complex (Fig. 4). These nodes reflect the

general pattern of enrichment in components relating to cell structure (e.g., podosome, sarcomere, collagen trimer, actin cytoskeleton) and mitochondria (five GO terms specifically related to mitochondrial structure, as well as oxidoreductase complex).

For Molecular Functions, a total of 30 GO terms were enriched, with 15 and 16 terms for each of up- and down-regulated proteins, with protein-containing complex binding commonly enriched by both groups of DA proteins.

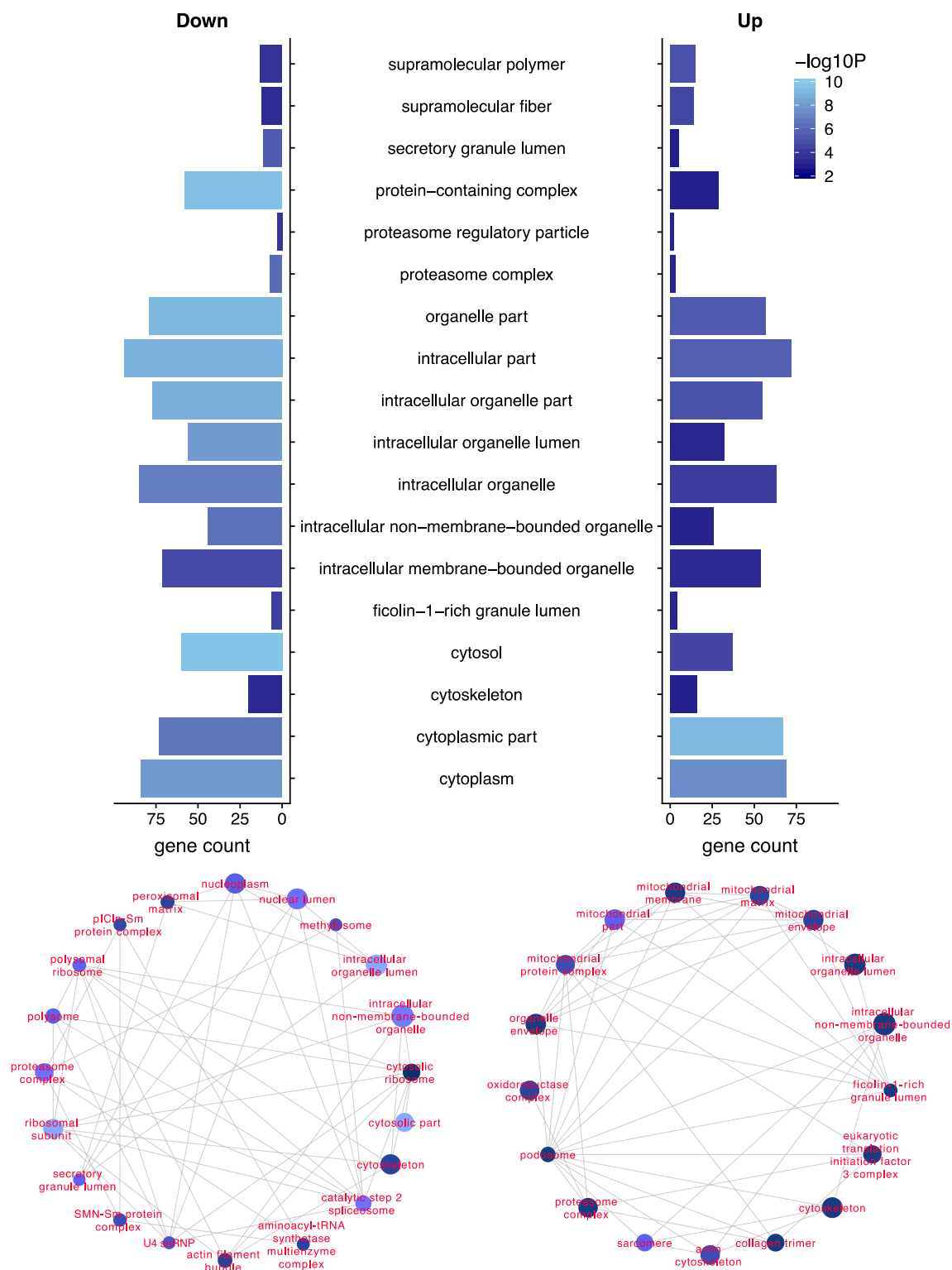


**Fig. 4** Functional networks of enriched GO terms within Cellular Components. The 18 commonly enriched terms for proteins that were up- and down-regulated in juvenile relative to embryonic hearts are compared (top) with respect to the number of differentially abundant

proteins included in each term (gene count) and the enrichment score ( $-\log_{10} P$ ). The uniquely enriched GO terms are shown as networks below for down-regulated (left) and up-regulated (right) proteins

Functional networks generated from these GO terms were sparsely populated, but generally related to actin binding, oxidoreductase activity, and peptidase activity up-regulated proteins; and to nucleic acid binding for down-regulated proteins (Supplemental Fig. S2).

## Discussion

This is the first description of the ontogenic changes to the cardiac proteome of American alligators. During the first 2 years of life, relative steady-state protein expression in the heart shifts between an embryonic heart that is primarily devoted to protein synthesis, to a maturing juvenile heart with increased capacity for muscle contraction and aerobic energy production. Not surprisingly, these results suggest that cellular investment shifts during development from growth to maintenance; however, as discussed below, these changes occur far slower than in birds where endothermy imposes substantially higher demands on the heart. What stands out in the alligator heart, however, is that the developmental program required for cardiac growth and maturation is largely resistant to a potent abiotic stressor, hypoxia (Alderman et al. 2019), which is known to drive pathogenic developmental programming in the hearts of placental mammals (McMillen and Robinson 2005; Patterson and Zhang 2010; Giussani and Davidge 2013; Ducsay et al. 2018).

The cardiac proteome of embryonic alligator hearts revealed significant enrichment of pathways related to protein synthesis, from transcription through translation, relative to hearts of 2-year-old juveniles. This suggests that, even as the embryo is nearing hatch, the heart is still investing most of its resources into tissue building rather than maturation, and may indicate that a significant population of replicating embryonic stem cells are still present in the embryonic heart. For example, mammalian embryonic stem cells have a comparatively higher proliferation rate than differentiating cardiomyocytes, and this is coincident with increased expression of genes and proteins involved in protein synthesis, including ribosomal and translation initiation factors (Richards 2004; Osman et al. 2010). While there is currently no histological description of cell and tissue morphology of the developing alligator heart, the enrichment of pathways involved in protein synthesis suggests tissue growth via hyperplasia. Interestingly, absolute heart mass of embryonic alligators does not change during the 1st month post-hatch (Sirsat et al. 2016b), nor is there an increase in relative heart mass up to 3 years later (Galli et al. 2016; Sirsat et al. 2016b), so any hyperplastic or hypertrophic growth occurs at a slow rate.

By 2 years post-hatch, the cardiac proteome divested away from protein synthesis towards a maturation stage where high rates of protein synthesis may no longer be

required to meet the basic maintenance of cardiac tissue. The maturing cardiac phenotype includes greater steady-state expression of sarcomeric proteins, and this increase in the relative proportion of functioning myofilament in the cardiomyocytes would increase their force-generating capacity. As their contractile function increases, so too does the biomechanical force experienced by the myocytes. The enrichment of GO terms for collagen trimer, cytoskeletal actin, and podosomes suggests the juvenile heart has enhanced its structural integrity alongside its contractile capacity. These changes mirror the early proteome changes associated with exercise training in rainbow trout (Dindia et al. 2017) that, over time, result in improved aerobic performance (Greer Walker and Emerson 1978; Davie et al. 1986; Gallagher et al. 2001; Castro et al. 2013).

Crossbridge cycling dynamics depend on ATP supply. The cardiac proteome of 2-year-old alligators provides strong evidence for mitochondrial biogenesis (Fig. 4), suggesting enhanced capacity for oxidative phosphorylation in the maturing heart. The onset of mitochondrial biogenesis is likely delayed considerably post-hatch, since no difference in mass-specific capacity for oxidative phosphorylation was observed in isolated mitochondria of hearts from 90% development through to 1 year (Sirsat et al. 2016a). In 3-year-old juvenile hearts, however, the mass-specific capacity for oxidative phosphorylation was nearly double that of mitochondria from embryonic hearts, and coincided with increased maximal activity of citrate synthase (Galli et al. 2016). The changes in alligator heart development are quite different from that of a precocial bird, the Peking duck (*Anas platyrhynchos domestica*), where early post-hatch life is marked by the onset of thermoregulation (Sirsat et al. 2016a). The duck heart undergoes substantial growth in the first few days after hatch to meet the metabolic demands of endothermy, including a sixfold increase in absolute heart mass by 7 days (Sirsat et al. 2016a). For comparison, the relative heart mass of a 7-day-old duckling is 3.5-fold greater than that of a 3-year-old alligator (Galli et al. 2016; Sirsat et al. 2016a), highlighting the significant role of the cardiovascular system in supporting endothermy. During this same developmental period, the mass-specific capacity for oxidative phosphorylation in isolated mitochondria from the duckling heart increased by approximately 60% (Sirsat et al. 2016a), achieving maximal rates that far exceed those of juvenile alligators (Galli et al. 2016; Sirsat et al. 2016b).

While alligators may experience an increase in aerobically fuelled crossbridge cycling as the heart matures to 2 years and beyond, the relatively low demand imposed on the heart by these slow-growing, sit-and-wait ectotherms means that the required changes in protein expression can occur at a slow pace relative to that of endotherms. This could offer an advantage of improving the tolerance of the cardiac phenotype to variation in abiotic factors, such as oxygen. Large



reptiles, including alligators, bury large clutches of eggs in subterranean or mound nests. This creates a natural barrier to oxygen diffusion that may be exacerbated during incubation as embryo mass increases (Tate et al. 2016). Importantly, the changes in the cardiac proteome described in the present study occurred independently of two different embryonic incubation regimes in the lab—one in regular 21% O<sub>2</sub> saturation, and the other at a realistic level of hypoxia, 10% O<sub>2</sub> saturation (Alderman et al. 2019). Embryonic hypoxia exposure nevertheless influenced the expression of 145 cardiac proteins (Alderman et al. 2019) that provide a mechanistic explanation for many of the known morphological and functional changes induced by developmental hypoxia in alligators (Galli et al. 2016; Tate et al. 2016; Joyce et al. 2018), yet the magnitude of this response (26% of total) was lower than the proteomic changes associated with development alone (74% of total). This demonstrates a robust cardiac ontogenic program that is buffered against, or protected from, variation in embryonic conditions in the nest. This may relate to the importance of hatching synchrony in reptilian egg clutches, where individual survival is greatly enhanced if the clutch emerges en masse (Vergne and Mathevon 2008; Doody 2011; McGlashan et al. 2018). In fact, some reptiles use heart rates of their clutch mates as a developmental cue to increase or decrease development rate, helping to synchronize hatch times (Vergne and Mathevon 2008), which offers some rationale for the robust nature of the cardiac proteome during early life in American alligators. It would be interesting to determine whether the cardiac proteome is equally robust against other abiotic factors that can influence developmental rate or cardiac function, such as temperature and environmental contaminants.

**Acknowledgements** We would like to acknowledge Derek Nelson, Justin Conner, Amanda Reynolds and Janna Crossley for their contribution to animal care. The authors wish to thank Jonathan Krieger of SPARC BioCentre Molecular Analysis, The Hospital for Sick Children, Toronto, Canada for assistance with iTRAQ analysis. D.A.C.II. is supported by a University of North Texas Office of Research and Innovation award and by a National Science Foundation CAREER award IBN IOS-0845741. T.E.G. is supported by a Natural Sciences and Engineering Research Council (NSERC) of Canada Discovery Grant (No. 71489) and an NSERC Discovery Accelerator Supplement.

**Author contributions** DACII, SLA, and TEG conceived the experiments; DACII and SLA conducted the experiments; SLA and TEG analyzed the results; RME provided alligator eggs. All authors reviewed the manuscript.

## References

- Agbulut O, Noirez P, Beaumont F, Butler-Browne G (2003) Myosin heavy chain isoforms in postnatal muscle development of mice. *Biol Cell* 95:399–406. [https://doi.org/10.1016/S0248-4900\(03\)00087-X](https://doi.org/10.1016/S0248-4900(03)00087-X)
- Alderman SL, Dindia LA, Kennedy CJ et al (2017) Proteomic analysis of sockeye salmon serum as a tool for biomarker discovery and new insight into the sublethal toxicity of diluted bitumen. *Comp Biochem Physiol Part D Genomics Proteomics* 22:157–166. <https://doi.org/10.1016/j.cbd.2017.04.003>
- Alderman SL, Crossley DA, Elsey RM, Gillis TE (2019) Hypoxia-induced reprogramming of the cardiac phenotype in American alligators (*Alligator mississippiensis*) revealed by quantitative proteomics. *Sci Rep* 9:8592. <https://doi.org/10.1038/s41598-019-45023-3>
- Anderson PAW, Glick KL, Manring A, Crenshaw C (1984) Developmental changes in cardiac contractility in fetal and postnatal sheep: in vitro and in vivo. *Am J Physiol Hear Circ Physiol* 16:H371–H379
- Berger PJ, Horne RS, Soust M et al (1990) Breathing at birth and the associated blood gas and pH changes in the lamb. *Respir Physiol* 82:251–265. [https://doi.org/10.1016/0034-5687\(90\)90039-2](https://doi.org/10.1016/0034-5687(90)90039-2)
- Castro V, Grisdale-Helland B, Helland SJ et al (2013) Cardiac molecular-acclimation mechanisms in response to swimming-induced exercise in atlantic salmon. *PLoS ONE* 8:1–10. <https://doi.org/10.1371/journal.pone.0055056>
- Davie PS, Wells RM, Tetens V (1986) Effects of sustained swimming on rainbow trout muscle structure, blood oxygen transport, and lactate dehydrogenase isozymes: evidence for increased aerobic capacity of white muscle. *J Exp Zool* 237:159–171. <https://doi.org/10.1002/jez.1402370203>
- Dindia LA, Alderman SL, Gillis TE (2017) Novel insights into cardiac remodelling revealed by proteomic analysis of the trout heart during exercise training. *J Proteomics* 161:38–46. <https://doi.org/10.1016/j.jprot.2017.03.023>
- Doody JS (2011) Environmentally cued hatching in reptiles. *Integr Comp Biol* 51:49–61
- Ducsay CA, Goyal R, Pearce WJ et al (2018) Gestational hypoxia and developmental plasticity. *Physiol Rev* 98:1241–1334. <https://doi.org/10.1152/physrev.00043.2017>
- Dykes IM, van Bueren KL, Scambler PJ (2018) HIC2 regulates isoform switching during maturation of the cardiovascular system. *J Mol Cell Cardiol* 114:29–37. <https://doi.org/10.1016/j.yjmcc.2017.10.007>
- Fabiato A, Fabiato F (1978) Calcium-induced release of calcium from the sarcoplasmic reticulum of skinned cells from adult human, dog, cat, rabbit, rat, and frog hearts and from fetal and new-born rat ventricles. *Ann N Y Acad Sci* 307:491–522. <https://doi.org/10.1111/j.1749-6632.1978.tb41979.x>
- Gallaugh PE, Thorarensen H, Kiessling A, Farrell AP (2001) Effects of high intensity exercise training on cardiovascular function, oxygen uptake, internal oxygen transport and osmotic balance in chinook salmon (*Oncorhynchus tshawytscha*) during critical speed swimming. *J Exp Biol* 204:2861–2872
- Galli GLJ, Crossley J, Elsey RM et al (2016) Developmental plasticity of mitochondrial function in American alligators, *Alligator mississippiensis*. *Am J Physiol Regul Integr Comp Physiol* 311:R1164–R1172. <https://doi.org/10.1152/ajpregu.00107.2016>
- Giussani DA, Davidge ST (2013) Developmental programming of cardiovascular disease by prenatal hypoxia. *J Dev Orig Health Dis* 4:328–337. <https://doi.org/10.1017/S204017441300010X>
- Gokhin DS, Ward SR, Bremner SN, Lieber RL (2008) Quantitative analysis of neonatal skeletal muscle functional improvement in the mouse. *J Exp Biol* 211:837–843. <https://doi.org/10.1242/jeb.014340>
- Goldspink G, Ward PS (1979) Changes in rodent muscle fibre types during post-natal growth, undernutrition and exercise. *J Physiol* 296:453–469. <https://doi.org/10.1113/jphysiol.1979.sp013016>
- Greer Walker M, Emerson L (1978) Sustained swimming speeds and myotomal muscle function in the trout, *Salmo gairdneri*. *J Fish*

- Biol 13:475–481. <https://doi.org/10.1111/j.1095-8649.1978.tb03457.x>
- Hoerter J, Mazet F, Vassort G (1981) Perinatal growth of the rabbit cardiac cell: possible implications for the mechanism of relaxation. *J Mol Cell Cardiol* 13:725–740. [https://doi.org/10.1016/0022-2828\(81\)90255-8](https://doi.org/10.1016/0022-2828(81)90255-8)
- Hulbert AJ (1988) Metabolism and the development of endothermy. The developing marsupial. Springer, Berlin Heidelberg, pp 148–161
- Joyce W, Miller TE, Elsey RM et al (2018) The effects of embryonic hypoxic programming on cardiovascular function and autonomic regulation in the American alligator (*Alligator mississippiensis*) at rest and during swimming. *J Comp Physiol B Biochem Syst Environ Physiol* 188:967–976. <https://doi.org/10.1007/s00360-018-1181-2>
- Lopaschuk GD, Jaswal JS (2010) Energy metabolic phenotype of the cardiomyocyte during development, differentiation, and postnatal maturation. *J Cardiovasc Pharmacol* 56:130–140
- Lutz PL, Dunbar-Cooper A (1984) The nest environment of the American crocodile (*Crocodylus acutus*). *Copeia* 1984:153–161
- McGlashan JK, Thompson MB, Janzen FJ, Spencer R-J (2018) Environmentally induced phenotypic plasticity explains hatching synchrony in the freshwater turtle *Chrysemys picta*. *J Exp Zool Part A Ecol Integr Physiol* 329:362–372. <https://doi.org/10.1002/jez.2217>
- McManus JJ (1971) Early postnatal growth and the development of temperature regulation in the mongolian gerbil, *Meriones unguiculatus*. *J Mammal* 52:782–792
- McMillen IC, Robinson JS (2005) Developmental origins of the metabolic syndrome: prediction, plasticity, and programming. *Physiol Rev* 85:571–633. <https://doi.org/10.1152/physrev.00053.2003>
- Mortola JP, Labbè K (2005) Oxygen consumption of the chicken embryo: interaction between temperature and oxygenation. *Respir Physiol Neurobiol* 146:97–106. <https://doi.org/10.1016/j.resp.2004.10.011>
- Nakanishi T, Jarmakani JM (1984) Developmental changes in myocardial mechanical function and subcellular organelles. *Am J Physiol* 246:H615–H625. <https://doi.org/10.1152/ajpheart.1984.246.4.H615>
- Osman AM, van Dartel DAM, Zwart E et al (2010) Proteome profiling of mouse embryonic stem cells to define markers for cell differentiation and embryotoxicity. *Reprod Toxicol* 30:322–332. <https://doi.org/10.1016/j.reprotox.2010.05.084>
- Patterson AJ, Zhang L (2010) Hypoxia and fetal heart development. *Curr Mol Med* 10:653–666. <https://doi.org/10.2174/156652410792630643>
- Posterino GS, Dunn SL, Botting KJ et al (2011) Changes in cardiac troponins with gestational age explain changes in cardiac muscle contractility in the sheep fetus. *J Appl Physiol* 111:236–243. <https://doi.org/10.1152/japplphysiol.00067.2011>
- Racca AW, Klaiman JM, Pioner JM et al (2016) Contractile properties of developing human fetal cardiac muscle. *J Physiol* 594:437–452. <https://doi.org/10.1113/JP271290>
- Richards M (2004) The transcriptome profile of human embryonic stem cells as defined by SAGE. *Stem Cells* 22:51–64. <https://doi.org/10.1634/stemcells.22-1-51>
- Robertson CE, Tattersall GJ, McClelland GB (2019) Development of homeothermic endothermy is delayed in high-altitude native deer mice (*Peromyscus maniculatus*). *Proc R Soc B Biol Sci* 286:20190841
- Sirsat SKG, Sirsat TS, Faber A et al (2016a) Development of endothermy and concomitant increases in cardiac and skeletal muscle mitochondrial respiration in the precocial Pekin duck (*Anas platyrhynchos domestica*). *J Exp Biol* 219:1214–1223. <https://doi.org/10.1242/jeb.132282>
- Sirsat SKG, Sirsat TS, Price ER, Dzialowski EM (2016b) Post-hatching development of mitochondrial function, organ mass and metabolic rate in two ectotherms, the American alligator (*Alligator mississippiensis*) and the common snapping turtle (*Chelydra serpentina*). *Biol Open* 5:443–451. <https://doi.org/10.1242/bio.017160>
- Snelling EP, Taggart DA, Maloney SK et al (2015a) Scaling of left ventricle cardiomyocyte ultrastructure across development in the kangaroo *Macropus fuliginosus*. *J Exp Biol* 218:1767–1776. <https://doi.org/10.1242/jeb.119453>
- Snelling EP, Taggart DA, Maloney SK et al (2015b) Biphasic allometry of cardiac growth in the developing Kangaroo *Macropus fuliginosus*. *Physiol Biochem Zool* 88:216–225. <https://doi.org/10.1086/679718>
- Tate KB, Rhen T, Eme J et al (2016) Periods of cardiovascular susceptibility to hypoxia in embryonic american alligators (*Alligator mississippiensis*). *Am J Physiol Regul Integr Comp Physiol* 310:R1267–R1278. <https://doi.org/10.1152/ajpregu.00320.2015>
- Thompson MB (2007) Comparison of the respiratory transition at birth or hatching in viviparous and oviparous amniote vertebrates. *Comp Biochem Physiol A Mol Integr Physiol* 148:755–760. <https://doi.org/10.1016/j.cbpa.2007.01.006>
- Tibbits GF, Xu L, Sedarat F (2002) Ontogeny of excitation-contraction coupling in the mammalian heart. *Comp Biochem Physiol A Mol Integr Physiol* 132:691–698. [https://doi.org/10.1016/s1095-6433\(02\)00128-9](https://doi.org/10.1016/s1095-6433(02)00128-9)
- Tyanova S, Temu T, Sinitcyn P et al (2016) The perseus computational platform for comprehensive analysis of (prote)omics data. *Nat Methods* 17:731–740
- Vergne AL, Mathevon N (2008) Crocodile egg sounds signal hatching time. *Curr Biol* 18:R513–R514
- Walter I, Seebacher F (2009) Endothermy in birds: underlying molecular mechanisms. *J Exp Biol* 212:2328–2336. <https://doi.org/10.1242/jeb.029009>

**Publisher's Note** Springer Nature remains neutral with regard to jurisdictional claims in published maps and institutional affiliations.